

Compendium of Current Single Event Effects for Candidate Spacecraft Electronics for NASA

Martha V. O'Bryan, Kenneth A. LaBel, Dakai Chen, Michael J. Campola, Megan C. Casey, Jean Marie Lauenstein, Jonathan A. Pellish, Raymond L. Ladbury, and Melanie D. Berg

Abstract — We present the results of single event effects (SEE) testing and analysis investigating the effects of radiation on electronics. This paper is a summary of test results.

Index Terms — Single event effects, spacecraft electronics, digital, linear bipolar, and hybrid devices

I. INTRODUCTION

NASA spacecraft are subjected to a harsh space environment that includes exposure to various types of ionizing radiation. The performance of electronic devices in a space radiation environment are often limited by their susceptibility to single event effects (SEE). Ground-based testing is used to evaluate candidate spacecraft electronics to determine risk to spaceflight applications. Interpreting the results of radiation testing of complex devices is challenging. Given the rapidly changing nature of technology, radiation test data are most often application-specific and adequate understanding of the test conditions is critical [1].

Studies discussed herein were undertaken to establish the application-specific sensitivities of candidate spacecraft and emerging electronic devices to single-event upset (SEU), single-event latchup (SEL), single-event gate rupture (SEGR), single-event burnout (SEB), and single-event transient (SET).

For total ionizing dose (TID) and displacement damage dose (DDD) results, see a companion paper submitted to the 2015 Institute of Electrical and Electronics Engineers (IEEE) Nuclear and Space Radiation Effects Conference (NSREC) Radiation Effects Data Workshop (REDW) entitled "Compendium of Current Total Ionizing Dose and Displacement Damage for Candidate Spacecraft Electronics for NASA" by M. Campola, *et al.* [2].

This work was supported in part by the NASA Electronic Parts and Packaging Program (NEPP), NASA Flight Projects, and the Defense Threat Reduction Agency (DTRA).

Martha V. O'Bryan, and Melanie D. Berg are with ASRC Federal Space and Defense, Inc. (AS&D, Inc.), 7515 Mission Drive, Suite 200, Seabrook, MD 20706, work performed for NASA Goddard Space Flight Center (GSFC), emails: martha.v.obryan@nasa.gov and Melanie.D.Berg@nasa.gov.

II. TEST TECHNIQUES AND SETUP

A. Test Facilities

All tests were performed between February 2014 and February 2015. Heavy ion experiments were conducted at the Lawrence Berkeley National Laboratory (LBNL) [3] and at the Texas A&M University Cyclotron (TAMU) [4]. Both of these facilities provide a variety of ions over a range of energies for testing. Each device under test (DUT) was irradiated with heavy ions having linear energy transfer (LET) ranging from 0.6 to 120 MeV•cm²/mg. Fluxes ranged from 1x10² to 1x10⁵ particles/cm²/s, depending on device sensitivity. Representative ions used are listed in Tables I and II. LETs in addition to the values listed were obtained by changing the angle of incidence of the ion beam with respect to the DUT, thus changing the path length of the ion through the DUT and the "effective LET" of the ion [5]. Energies and LETs available varied slightly from one test date to another.

Laser SEE tests were performed at the pulsed laser facility at the Naval Research Laboratory (NRL) [6], [7]. Single photon absorption method was used with the laser light having a wavelength of 590 nm resulting in a skin depth (depth at which the light intensity decreased to 1/e – or about 37% – of its intensity at the surface) of 2 μm. A nominal pulse rate of 1 kHz was utilized. Pulse width was 1 ps, beam spot size ~1.2 μm.

TABLE I: LBNL TEST HEAVY IONS

Ion	Energy (MeV)	Surface LET in Si (MeV•cm ² /mg) (Normal Incidence)	Range in Si (μm)
¹⁸ O	183	2.2	226
²² Ne	216	3.5	175
⁴⁰ Ar	400	9.7	130
²³ V	508	14.6	113
⁶⁵ Cu	660	21.2	108
⁸⁴ Kr	906	30.2	113
¹⁰⁷ Ag	1039	48.2	90
¹²⁴ Xe	1233	58.8	90
LBNL 10 MeV per amu tune			

Kenneth A. LaBel, Dakai Chen, Michael J. Campola, Megan C. Casey, Jean-Marie Lauenstein, Jonathan A. Pellish, and Raymond L. Ladbury are with NASA/GSFC, Code 561.4, Greenbelt, MD 20771 (USA), emails: kenneth.a.label@nasa.gov, Dakai.Chen-1@nasa.gov, michael.j.campola@nasa.gov, megan.c.casey@nasa.gov, jonathan.a.pellish@nasa.gov, jean.m.lauenstein@nasa.gov, raymond.l.ladbury@nasa.gov.

TABLE III: TAMU TEST HEAVY IONS

Ion	Energy (MeV)	Surface LET in Si (MeV•cm ² /mg) (Normal Incidence)	Range in Si (μm)
⁴ He	98	0.07	3401
¹⁴ N	210	1.3	428
²⁰ Ne	300	2.5	316
⁴⁰ Ar	599	7.7	229
⁶³ Cu	944	17.8	172
⁸⁴ Kr	1259	25.4	170
¹⁰⁹ Ag	1634	38.5	156
¹²⁹ Xe	1934	47.3	156
¹⁹⁷ Au	2954	80.2	155
TAMU 15 MeV per amu tune			
⁸⁴ Kr	2081	19.8	332
¹³⁹ Xe	3197	38.9	286
TAMU 25 MeV per amu tune			

amu = atomic mass unit

B. Test Method

Unless otherwise noted, all tests were performed at room temperature and with nominal power supply voltages. Device qualification include SEL high-temperature, V_{CC} plus worst-case and for SEU/SET high-temperature, V_{CC} minus worst-case. Unless otherwise noted, SEE testing was performed in accordance with JESD57 test procedures where applicable [8].

1) SEE Testing - Heavy Ion:

Depending on the DUT and the test objectives, one or more of three SEE test approaches were typically used:

Dynamic – the DUT was continually exercised while being exposed to the beam. The events and/or bit errors were counted, generally by comparing the DUT output to an unirradiated reference device or with an expected output (Golden chip or virtual Golden chip methods) [9]. In some cases, the effects of clock speed or device operating modes were investigated. *Results of such tests should be applied with caution due to their application-specific nature.*

Static – the DUT was configured prior to irradiation; data were retrieved and errors were counted after irradiation.

Biased – the DUT was biased and clocked while power consumption was monitored for SEL or other destructive effects. In most SEL tests, functionality was also monitored.

DUTs were monitored for soft errors, such as SEUs, and for hard failures, such as SEGR. Detailed descriptions of the types of errors observed are noted in the individual test reports [10], [11].

SET testing was performed using high-speed oscilloscopes controlled via LabVIEW®. Individual criteria for SETs are specific to the device and application being tested. Please see the individual test reports for details [10], [11].

Heavy ion SEE sensitivity experiments include measurement of the linear energy transfer threshold (LET_{th}) and cross section at the maximum measured LET. The LET_{th} is defined as the maximum LET value at which no effect was observed at an effective fluence of 1×10^7 particles/cm². In the case where events are observed at the smallest LET tested, LET_{th} will either be reported as less than the lowest measured LET or determined approximately as the LET_{th} parameter from a Weibull fit. In the case of SEGR experiments, measurements are made of the SEGR threshold V_{ds} (drain-to-source voltage) as a function of LET and ion energy at a fixed V_{gs} (gate-to-source voltage).

2) SEE Testing - Pulsed Laser

The DUT was mounted on an X-Y-Z stage in front of a 100x lens that produces a spot diameter of approximately 1 μm at full-width half-maximum (FWHM). The X-Y-Z stage can be moved in steps of 0.1 μm for accurate determination of SEU sensitive regions in front of the focused beam. An illuminator, together with a charge coupled device (CCD) camera and monitor, were used to image the area of interest thereby facilitating accurate positioning of the device in the beam. The pulse energy was varied in a continuous manner using a polarizer/half-waveplate combination and the energy was monitored by splitting off a portion of the beam and directing it at a calibrated energy meter.

III. TEST RESULTS OVERVIEW

Principal investigators are listed in Table III. Abbreviations and conventions are listed in Table IV. SEE results are summarized in Table V. Unless otherwise noted all LETs are in MeV•cm²/mg and all cross sections are in cm²/device. All SEL tests are performed to a fluence of 1×10^7 particles/cm² unless otherwise noted.

TABLE III: LIST OF PRINCIPAL INVESTIGATORS

Principal Investigator (PI)	Abbreviation
Melanie D. Berg	MB
Megan C. Casey	MCC
Michael J. Campola	MiC
Dakai Chen	DC
Raymond L. Ladbury	RL
Jean-Marie Lauenstein	JML
Jonathan A. Pellish	JP

TABLE IV: ABBREVIATIONS AND CONVENTIONS

LET = linear energy transfer (MeV•cm²/mg)
LET_{th} = linear energy transfer threshold (the maximum LET value at which no effect was observed at an effective fluence of 1x10⁷ particles/cm² – in MeV•cm²/mg)
< = SEE observed at lowest tested LET
> = no SEE observed at highest tested LET
σ = cross section (cm²/device, unless specified as cm²/bit)
σ_{maxm} = cross section at maximum measured LET (cm²/device, unless specified as cm²/bit)
ADC = analog to digital converter
BiCMOS = bipolar complementary metal oxide semiconductor
CMOS = complementary metal oxide semiconductor
DUT = device under test
ECC = error correcting code
eng samples = engineering samples
GPIB = general purpose interface bus
H = heavy ion test
ID# = identification number
I_{ds} = drain-source leakage current
I_{out} = output current
L = laser test
LBNL = Lawrence Berkeley National Laboratory
LDC = lot date code
min = minimum
MLC = multiple-level cell
MOSFET = metal-oxide-semiconductor field-effect transistor
NAND = Negated AND or NOT AND
NRL = Naval Research Laboratory

PCB = printed circuit board
PECL = positive emitter coupled logic
PI = principal investigator
PIGS = post-irradiation gate stress
pkg = package
PNP = positive-negative-positive
REAG = radiation effects and analysis group
SBU = single-bit upset
SEB = single event burnout
SEE = single event effect
SEFI = single-event functional interrupt
SEGR = single event gate rupture
SEL = single event latchup
SET = single event transient
SEU = single event upset
SiC = silicon carbide
SiGe = silicon germanium
SMART = self-monitoring, analysis and reporting technology
SSD = solid state drive
SSR = solid state relay
TAMU = Texas A&M University Cyclotron Facility
V_{CC} = power supply voltage
VDMOS = vertical double diffused MOSFET
V_{ds} = drain-to-source voltage
V_{gs} = gate-to-source voltage
VNAND = vertical-NAND
Xe = Xenon

TABLE V: SUMMARY OF SEE TEST RESULTS

Part Number	Manufacturer	REAG ID#; LDC or Wafer #	Device Function	Technology	Particle: (Facility/Year/Month) P.I.	Test Results: LET in MeV•cm ² /mg, σ in cm ² /device, unless otherwise specified	Supply Voltage	Sample Size (Number Tested)
Memory Devices:								
RM24	Adesto	13-082; No LDC	CBRAM	NonVolatile Memory	H: (LBNL14May; LBNL14Sep) DC L: (NRL14Jun) DC	H: SEL LET _{th} >83; 10 < SEU LET _{th} < 20; SEFI LET _{th} < 7.3; SEFI σ=5.9x10 ⁻⁷ cm ² at LET 83; SEFIs can be recovered via power cycle in most cases, rewrite was required in some cases. Bit upsets were only observed in write/read mode. L: Laser test identified areas on the die that are sensitive to SEFI: bandgap reference, voltage regulator, SRAM, and logic circuits. [12], [13]	2.7 to 3.6 V	4
850 PRO series MZ7KE256HMHA	Samsung	14-055, 14-056; No LDC	SSD	VNAND Flash Memory	H: (TAMU14Oct) DC	SEL LET _{th} >40; SEU LET _{th} < 1.8 SEFI LET _{th} < 1.8 SEFIs occurred during static and dynamic cycling test modes. Most SEFIs recoverable with power cycle. Some SEFIs caused data corruption, and required rewrite. Heavy ion-induced cell upsets were evident from reallocated sectors via ECC. [14], [15]	5 V	4
MN101L AM13L-STK2	Panasonic	13-075; No LDC	Microcontroller with Embedded Resistive Memory	ReRAM, 180 nm CMOS	H: (LBNL14May) DC; L: (NRL14Mar) DC	H: SEL LET _{th} > 70; 3.1 < SEFI LET _{th} < 4.4, σ = 4 × 10 ⁻⁵ cm ² /device at LET of 70. L: Pulsed-laser testing confirmed the SEU tolerance of the resistive memory array, and identified the sense amplifier as a sensitive component for SEFIs. [16]	3.3V	3 at LBNL; 1 at NRL
Linear/Mixed Signal Devices:								
LM6172	Texas Instruments	13-076; 1208A	Operational Amplifier	Bipolar	H: (TAMU13Dec; TAMU14Apr) MCC	SET 0.14 < LET _{th} < 0.87; σ _{maxm} = 1x10 ⁻³ cm ² . [17]	±5 V	2 (2013); 3 (2014)
AD7984	Analog Devices	14-053; C60	ADC	Bipolar	H: (TAMU14Oct) MiC	SEL LET _{th} > 75.1; SET of 60 μs at LET >28.8 for given application. [18]	2.5 V	4
MAX4595DVBR	Texas Instruments	14-077; pkg info SOT-23 6SB	Analog Switch	CMOS	H: (TAMU14Oct) MiC	SEL LET _{th} > 85; negative transients were observed ~2.5 μs long and -750 mV in amplitude; worst transient observed was 10 μs long and had negative going amplitudes of less than 1.5 V at LET 27.8 [19]	3.3V, 5V, 6V	3
MAX308ESE	Maxim	14-061; 1108	Analog Multiplexer	CMOS	H: (TAMU14Oct) MiC	SEL LET _{th} > 89 [20]	+/-15V	1

Part Number	Manufacturer	REAG ID#, LDC or Wafer #	Device Function	Technology	Particle: (Facility/Year/Month) P.I.	Test Results: LET in MeV·cm ² /mg, σ in cm ² /device, unless otherwise specified	Supply Voltage	Sample Size (Number Tested)
TLV5618	Texas Instruments	14-070; 0801A	ADC	CMOS	H: (TAMU14Oct) RL	8.1 < SEL LET _{th} < 11.4 σ_{max} ~ 6x10 ⁻⁵ cm ² ; SET LET _{th} < 1.8, σ_{max} ~ 2x10 ⁻⁴ cm ² ; 3.6 < SEU LET _{th} < 5.5, σ_{max} ~ 1.5x10 ⁻⁵ cm ² . [21]	5 V; 6 V	2
ADP3330	Analog Devices	14-074; 1238	Voltage Regulator	BiCMOS	H: (TAMU14Oct) RL	SEL LET _{th} > 53.1; 28.8 < SET LET _{th} < 53.1, σ_{max} ~ 1.5x10 ⁻⁵ cm ² ; packaging precluded testing at angle. [22]	3.3 V	2
LMV7219	Texas Instruments	14-072; 1249	Comparator	BiCMOS	H: (TAMU14Oct) RL	SEL LET _{th} > 53.1; SET LET _{th} < 2.8, σ not saturated at LET=53.1; LET and cross section depend on input voltage ΔV_{in} ; transients can last up to several microseconds. [23]	5 V	3
AZ88923	Arizona Microtek	14-073 0146	Integrated Circuit	SiGe PECL	H: (TAMU15Oct) RL	SETs with durations up to 10 microseconds were observed at LET ~ 17. SET LET _{th} < 1.8; SET σ_{max} 1.1x10 ⁻⁴ cm ² . [24]	3.3 V	3
Power Device:								
SMHF2812	Crane Interpoint	14-021; 1021, 1214	DC-DC Converter	Hybrid	H: (TAMU14Jul) MCC	No destructive SEEs observed at 44 MeV-cm ² /mg in either LDC. [25]	28 V, 35 V	6
CMF10120D	CREE	12-080; W52812	MOSFET	SiC VDMOS	H: (LBNL14Sept) JML; MCC	966-MeV Xe (LET=65 in SiC): min evaluated V _{ds} =182 V: Failed Idss and PIGS tests; at higher V _{ds} , primary failure mode SEB. [26]	0 V _{GS}	11
SCT30N120	STMicroelectronics	14-050; No LDC (eng samples)	SiC MOSFETs	SiC VDMOS	H: (LBNL14June) JML	Contact PI for test results.	0 V _{GS}	24
Diodes – Pass at 100% of Reverse Voltage:								
FYPF2010DN	Fairchild Semiconductor	14-032; E13AA wafer	Diode	Si	H: (LBNL14June) MCC	No failures observed at 100% of reverse voltage when irradiated with 1233 MeV Xe (LET = 58.8). [27], [28]	100 V	3
MBR4045WT	ON Semiconductor	14-040; NFB19G wafer	Diode	Si	H: (LBNL14June) MCC	No failures observed at 100% of reverse voltage when irradiated with 1233 MeV Xe (LET = 58.8). [27], [28]	45 V	3
RB205T-60	Rohm Semiconductor	14-023; No LDC	Diode	Si	H: (LBNL14June) MCC	No failures observed at 100% of reverse voltage when irradiated with 1233 MeV Xe (LET = 58.8). [27], [28]	60 V	3
MBR4045CT	Vishay	14-025; P350X wafer	Diode	Si	H: (LBNL14June) MCC	No failures observed at 100% of reverse voltage when irradiated with 1233 MeV Xe (LET = 58.8). [27], [28]	45 V	3
Diodes – Degradation and Pass at 100% of Reverse Voltage:								
MBR2080CT	ON Semiconductor	14-043; NF914 wafer	Diode	Si	H: (LBNL14June) MCC	Degradation observed during beam run while biased at 100% of reverse voltage, but all parameters remained within specification when irradiated with 1233 MeV Xe (LET = 58.8). [27], [28]	80 V	3
Diodes – Degradation and Failure at 100% of Reverse Voltage:								
MBRF2045CT	ON Semiconductor	14-039; SPB17 wafer	Diode	Si	H: (LBNL14June) MCC	Degradation observed during beam run while biased at 75% of reverse voltage, but all parameters remained within specification when irradiated with 1233 MeV Xe (LET = 58.8). Degradation was also observed during beam run when biased at 100% of reverse voltage, but parameters exceeded specification. [27], [28]	45 V	4
MBR6045WT	ON Semiconductor	14-041; NFE04G wafer	Diode	Si	H: (LBNL14June) MCC	Degradation observed during beam run while biased at 75% of reverse voltage, but all parameters remained within specification when irradiated with 1233 MeV Xe (LET = 58.8). Degradation was also observed during beam run when biased at 100% of reverse voltage, but parameters exceeded specification. [27], [28]	45 V	4
Diodes – Catastrophic Failure at 100% of Reverse Voltage:								
MBRF20100CT	ON Semiconductor	14-044; SPB16 wafer	Diode	Si	H: (LBNL14June) MCC	No failures observed at 75% of reverse voltage when irradiated with 1233 MeV Xe (LET = 58.8). Catastrophic failure was observed at 100% of reverse voltage. [27], [28]	100 V	3
STPS20200C	STMicroelectronics	14-037; 640DN wafer	Diode	Si	H: (LBNL14June) MCC	No failures observed at 75% of reverse voltage when irradiated with 1233 MeV Xe (LET = 58.8). Catastrophic failure was observed at 100% of reverse voltage. [27], [28]	200 V	4

Part Number	Manufacturer	REAG ID#, LDC or Wafer #	Device Function	Technology	Particle: (Facility/Year/Month) P.I.	Test Results: LET in MeV•cm ² /mg, σ in cm ² /device, unless otherwise specified	Supply Voltage	Sample Size (Number Tested)
MBR20100CT	Fairchild Semiconductor	14-031; A1250 wafer	Diode	Si	H: (LBNL14June) MCC	Degradation observed during beam run while biased at 75% of reverse voltage, but all parameters remained within specification when irradiated with 1233 MeV Xe (LET = 58.8). Catastrophic failures observed when biased at 100% of reverse voltage. [27], [28]	100 V	3
MBR20200CT	Fairchild Semiconductor	14-033; A1034 wafer	Diode	Si	H: (LBNL14June) MCC	Degradation observed during beam run while biased at 75% of reverse voltage, but all parameters remained within specification when irradiated with 1233 MeV Xe (LET = 58.8). Catastrophic failures observed when biased at 100% of reverse voltage. [27], [28]	200 V	3
NXPS20H100CX	NXP Semiconductor	14-022; 1310	Diode	Si	H: (LBNL14June) MCC	Degradation observed during beam run while biased at 75% of reverse voltage, but all parameters remained within specification when irradiated with 1233 MeV Xe (LET = 58.8). Catastrophic failures observed when biased at 100% of reverse voltage. [27], [28]	100 V	3
MBR2060CT	ON Semiconductor	14-042; NF031 wafer	Diode	Si	H: (LBNL14June) MCC	Degradation observed during beam run while biased at 75% of reverse voltage, but all parameters remained within specification when irradiated with 1233 MeV Xe (LET = 58.8). Catastrophic failures observed when biased at 100% of reverse voltage. [27], [28]	60 V	3
STPS30H100C	STMicroelectronics	14-036; 7SAGG wafer	Diode	Si	H: (LBNL14June) MCC	Degradation observed during beam run while biased at 75% of reverse voltage, but all parameters remained within specification when irradiated with 1233 MeV Xe (LET = 58.8). Catastrophic failures observed when biased at 100% of reverse voltage. [27], [28]	100 V	3
STPS60SM200C	STMicroelectronics	14-038; G406X wafer	Diode	Si	H: (LBNL14June) MCC	Degradation observed during beam run while biased at 75% of reverse voltage, but all parameters remained within specification when irradiated with 1233 MeV Xe (LET = 58.8). Catastrophic failures observed when biased at 100% of reverse voltage. [27], [28]	200 V	3
MBR20100CT	Vishay	14-026; 1411G wafer	Diode	Si	H: (LBNL14June) MCC	Degradation observed during beam run while biased at 75% of reverse voltage, but all parameters remained within specification when irradiated with 1233 MeV Xe (LET = 58.8). Catastrophic failures observed when biased at 100% of reverse voltage. [27], [28]	100 V	3
MBR60100	Vishay	14-027; 1335S wafer	Diode	Si	H: (LBNL14June) MCC	Degradation observed during beam run while biased at 75% of reverse voltage, but all parameters remained within specification when irradiated with 1233 MeV Xe (LET = 58.8). Catastrophic failures observed when biased at 100% of reverse voltage.	100 V	3
STPS40M60C	STMicroelectronics	14-035; 64OBY wafer	Diode	Si	H: (LBNL14June) MCC	No failures observed at 50% of reverse voltage when irradiated with 1233 MeV Xe (LET = 58.8). Degradation observed during beam run while biased at 75% of reverse voltage. Post-rad electrical parameter measurements were out of specification. Catastrophic failure was observed at 100% of reverse voltage. [27], [28]	60 V	4
MBR20H200CT	Vishay	14-028; 1330S wafer	Diode	Si	H: (LBNL14June) MCC	No failures observed at 50% of reverse voltage when irradiated with 1233 MeV Xe (LET = 58.8). Degradation observed during beam run while biased at 75% of reverse voltage. Post-rad electrical parameter measurements were out of specification. Catastrophic failure was observed at 100% of reverse voltage. [27], [28]	200 V	3
MBRC20200CT	ON Semiconductor	12-034; CH803691 S1 WFR#3	Diode	Si	H: (LBNL14June; Sept) MCC	Catastrophic failure was observed at 100% of reverse voltage when irradiated with 1233 MeV Xe (LET = 58.8). Elevated temperature does not appear to change part susceptibility. [27], [28]	200 V	3
STPS4045C	STMicroelectronics	14-034; 6K1F1 wafer	Diode	Si	H: (LBNL14June) MCC	No failures observed at 50% of reverse voltage when irradiated with 1233 MeV Xe (LET = 58.8). Catastrophic failure was observed at 75% and 100% of reverse voltage. [27], [28]	45 V	4
MBR3045PT	Fairchild Semiconductor	14-029; AC33 wafer	Diode	Si	H: (LBNL14June) MCC	Catastrophic failure was observed at 100% of reverse voltage when irradiated with 1233 MeV Xe (LET = 58.8). Additional testing is required. [27], [28]	45 V	4

Part Number	Manufacturer	REAG ID#, LDC or Wafer #	Device Function	Technology	Particle: (Facility/Year/Month) P.I.	Test Results: LET in MeV·cm ² /mg, σ in cm ² /device, unless otherwise specified	Supply Voltage	Sample Size (Number Tested)
FPGAs:								
A3PE3000L-PQ208 ProASIC	Microsemi	12-052; 1108	ProASIC FPGA	CMOS	H and P: (LBNL14May) MB	Ongoing research investigating different mitigation strategies. [29], [30]	1.5; 2.5; and 3.3 V	2
XC7K325T Kintex7	Xilinx	14-001; 1349	FPGA	CMOS	H: (TAMU14Apr/Oct/Dec) MB	SEU LET _{th} < 0.07 (configurable memory) [29], [30]	Varies w/data sheet	5
XQV5FX70T	Xilinx	14-015; 1774118	Virtex 5 FPGA	CMOS	H: (TAMU14Apr/Oct) MB	Contact PI for test results. [29], [30]	4.5 V	2
Test Chips:								
32 nm SOI (Deneb)	IBM	13-067; 14-013	SET Pulse Width Measurement	32 nm SOI CMOS	H: (LBNL14May) JP w/Rodbell	Contact Kenneth P. Rodbell [31]	0.9, nominal	1
Miscellaneous Devices:								
RDHA710	International Rectifier	14-008; 1340	Solid State Relay	Hybrid	H: (TAMU14Apr) MCC	SET LET _{th} < 87.1 MeV·cm ² /mg. No SEEs observed.	28 V, 35 V	2
RDHA701	International Rectifier	14-009; 1340	Solid State Relay	Hybrid	H: (TAMU14Apr) MCC	SET LET _{th} < 87.1 MeV·cm ² /mg. No SEEs observed.	28 V, 35 V	2

IV. TEST RESULTS AND DISCUSSION

As in our past workshop compendia of NASA Goddard Space Flight Center (GSFC) test results, each DUT has a detailed test report available online at <http://radhome.gsfc.nasa.gov> [11].

This section contains summaries of testing performed on a selection of featured parts.

A. Samsung 256 GB 850 Pro Solid State Drive

We evaluated the heavy ion single-event effect (SEE) susceptibility of the Samsung 850 PRO solid state drive (SSD). Their datasheets can be found on Samsung's websites [32], [33]. The 850 PRO drives consist of multiple-level cell (MLC) VNAND. The 256 GB SSD comprises 4 VNAND chips. Each chip consists of multiple stacked VNAND die. The other active components on the SSD, including the DDR3 memory and controller, were shielded during the beam exposure.

Fig. 1 shows a schematic of the test setup. The desktop PC for accessing the SSD is positioned in the irradiation chamber in close proximity to the device-under-test (DUT). The power supply is also positioned in the irradiation chamber. We remotely control the power supply via GPIB or USB interface.

We utilized an open source software called "Caine" as the diagnostic tool to perform read and write operations to the SSD [33]. The program interface also allows us to examine the Self-Monitoring, Analysis and Reporting Technology (SMART) attributes, which includes a list of reliability parameters for the SSD.

Fig. 2 shows a photograph of the test setup. The SSD operated in the static or dynamic test mode. In the static mode, we programmed the SSD with a pattern (00, FF, checkerboard), irradiated the device, read and recorded the bad addresses. In dynamic mode, we actively cycled in read or write/read mode and recorded errors during the exposure. In the event of a functional interrupt, we allowed the SSD to self-clear the error. If functionality did not recover, we cycled power to the SSD.

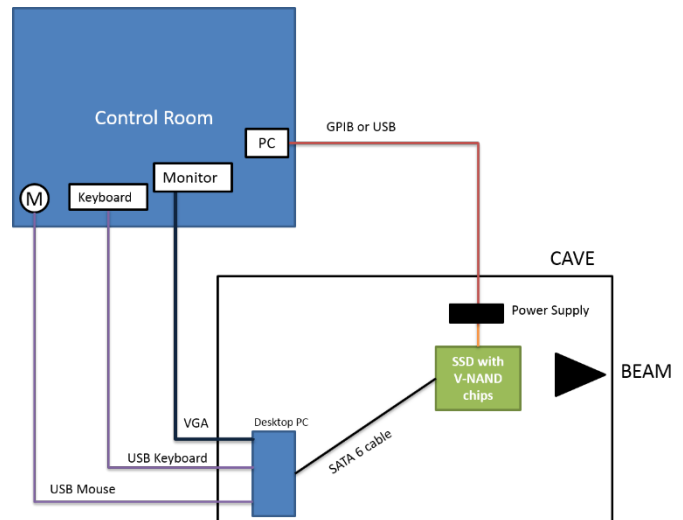


Fig. 1. Schematic diagram of the test setup.

Single-event functional interrupt (SEFI) dominated the SEE response. The SEFI LET threshold is less than 1.8 MeV·cm²/mg. The SSD recovered functionality by power reset in most cases, and the errors self-cleared on the second read in other cases. In addition, the SMART attributes revealed errors due to ion-induced cell corruption which were corrected by ECC.

Fig. 3 shows the SEFI cross section as a function of effective LET. The cross-section data have significant Poisson error, due to the low error count. We irradiated four parts with 25 MeV/amu Kr, Ar, and Ne, at various angles. The heavy ions likely penetrated multiple dies for some ion species (particularly Ne). Therefore, SEFI due to signal contention is possible. However, with that consideration, we carried out comparative runs with degraded beams, which reduced the ion penetration range to within one die, but still observed SEFIs with similar characteristics. Table VI categorizes the functional interrupt errors according to the device response, recovery method, and test mode. We note that the errors during

read/write tests occurred during the read cycle only. We did not detect write errors during the test.

Static on/off tests are representative of typical application conditions for storage flash devices. All of the SEEs that occurred during static mode testing caused the SSD to become nonresponsive. A power cycle was required to recover functionality following such an event. Critically, the SEFI occurred even when the SSD was unpowered during irradiation. The stored data were unaffected. We were able to successfully read the programmed data after a SEFI.

The program categorized the errors as either access errors or data corruption errors. The access errors meant that the SSD could not carry out the read successfully. The corrupt errors could represent radiation-induced corrupt cells. However, in some cases, the corrupt error could be cleared on a subsequent read. Thus they are likely caused by SEUs in the data buffers. However, cell corruption was evident in other cases. The SMART attribute, “reallocated sector count,” indicated the number of sectors which were removed and replaced due to cell corruption. The error count increased due to SEE even though the errors were not visible during read, since ECC detected and corrected the errant data by replacing the bad sectors.

Both read access errors and data corruption errors affected 8 continuous sectors (4 KB) at a time. The errors repeated every 128 sectors in most cases. The trend may reflect the data organization of the SSD, which we are not yet familiar with at the time of this writing. The 256 GB SSD consists of two 8 die chips and two 4 die chips. We irradiated the 8 die chip during the test. Assuming that the controller reads 4 KB from one die at a time, once the SSD encounters a SEFI, it skips the other dies in that chip and attempts to read from the next chip. Therefore, the total number of sectors from the other unirradiated chips should be $8 \times (4 + 4 + 8) = 128$ sectors. Consequently, we repeatedly observed the patterns of 8 continuous bad sectors followed by 128 error-free sectors. [14], [15]

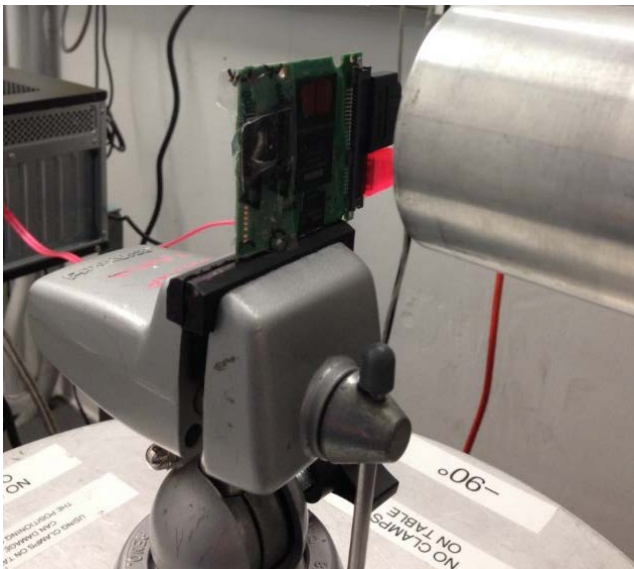


Fig. 2. Photograph of the test setup at the Texas A&M University Cyclotron facility. The printed circuit board is taken directly from the SSD. The exposed die is located near the top of the board. The other etched chip (left side on the board) is covered with a lid to avoid incidental exposure.

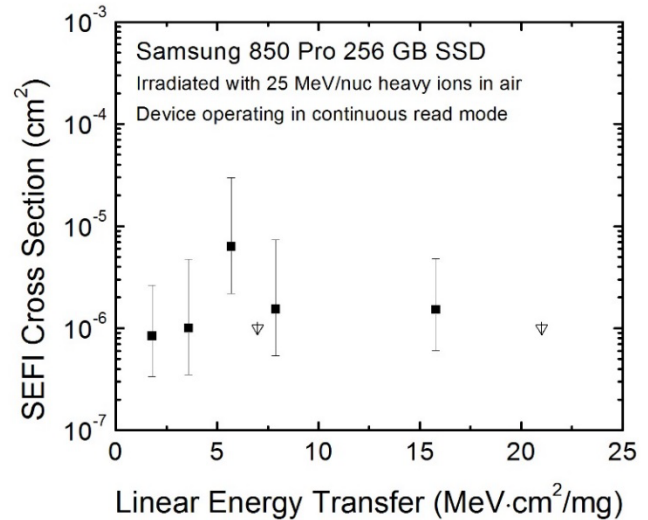


Fig. 3. SEFI cross section vs. LET for the 256 GB Samsung SSD irradiated with 25 MeV/amu heavy ions in air. Device was continuously read during irradiation. Arrows indicate maximum fluence levels without any observed error.

TABLE VI: SEFIS CATEGORIZED ACCORDING TO THE TEST MODE, EVENT CHARACTERISTICS, AND RECOVERY METHOD.

Test Mode	Description	Recovery method
Static on, Static off	SSD not responsive	Power cycle
Static on, Dynamic read	Read access errors	Power cycle, Self-cleared in one case
Dynamic read	Corrupt data errors with entire memory showing errors	Rewritten (Did not power cycle)
Dynamic read	Corrupt data errors with 8 continuous sectors showing errors	Self-cleared on next read

B. Texas Instruments LM6172 Operational Amplifier

The LM6172 is a matched pair of high speed, low power, low distortion voltage feedback amplifiers. It offers 100 MHz unity-gain bandwidth, 3000 V/μs slew rate and 50 mA of output current per channel, while consuming 2.3 mA of supply current per channel. The device can operate at ± 5 V or ± 15 V power supply. The LM6172 is built with Texas Instruments’ advanced VIP III (Vertically Integrated PNP).

Three parts were mechanically delidded. The parts were then soldered to small printed circuit boards (PCBs) that were designed specifically for this testing. The test circuits for one side of each device was configured as an inverter, while the other side was configured as a voltage follower. The inverter configuration was application specific for the instrument. Schematics of these circuit configurations are shown in the full test report [17].

While these parts showed no destructive SEEs, the LM6172 is highly susceptible to SETs. Fig. 4 shows the single-event transient cross section for transients with amplitude greater than

20 mV plotted on a log-linear scale. The blue data points show the application-specific inverter configuration, while the red points show the data from the voltage follower. The errors bars were calculated using Poisson statistics at the 90% confidence level. No transients were observed when irradiated with He, and these data points are indicated on the cross-section figures by a straight line with a downward-pointing arrow. Figs. 5 and 6 show the amplitudes and pulsewidths generated when irradiated with each ion in the inverter and voltage follower configurations, respectively. It should be noted that He is not shown on these figures because no transients were observed. Each ion is shown in a different color, while the different shapes indicate the angle of incidence used. The inverter configuration appears to very slightly lengthen the pulsewidth while reducing the transient amplitude. This is most likely due to the capacitance and resistance in the feedback loop which create an RC time constant that is not present in the voltage follower.

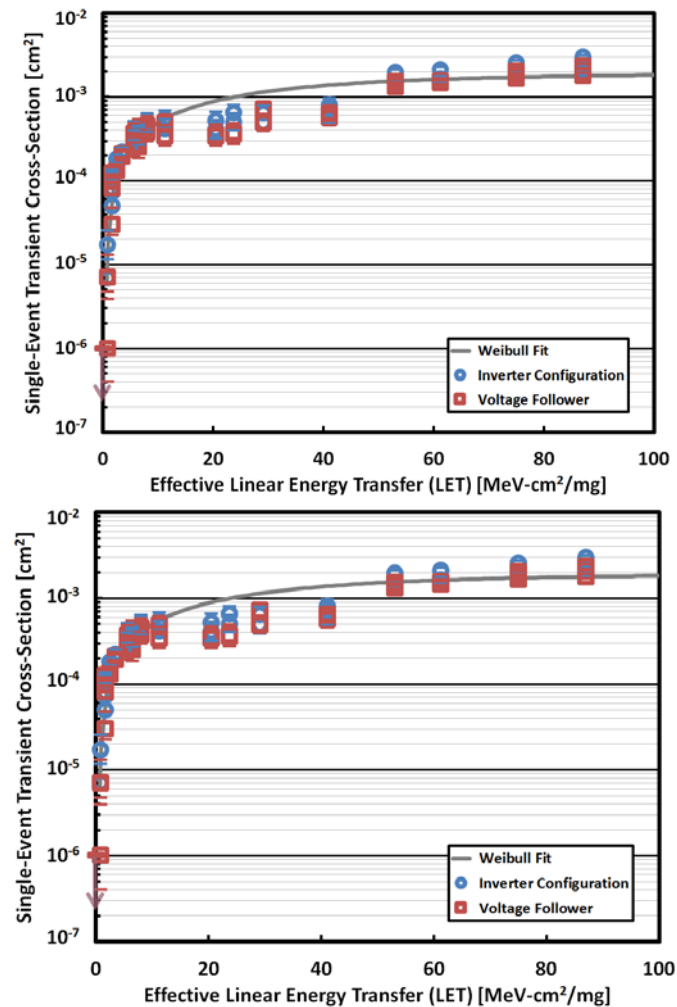


Fig. 4. Single-event transient cross-section as a function of effective LET for two LM6172 circuit configurations.

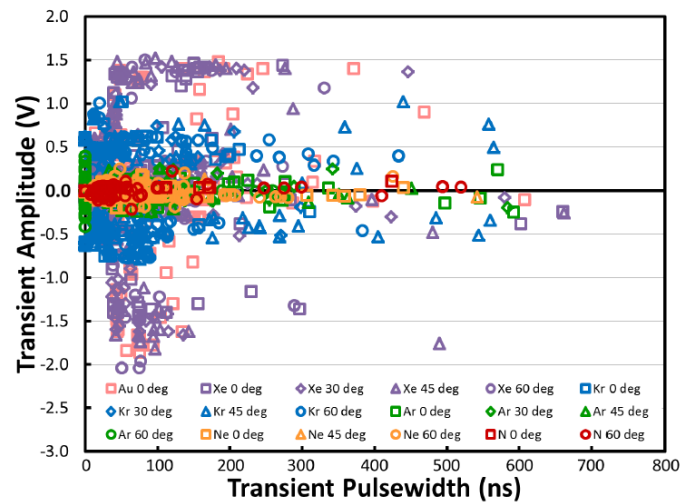


Fig. 5. Amplitude and pulsewidth scatterplot for transients generated on the LM6172 in the voltage follower configuration.

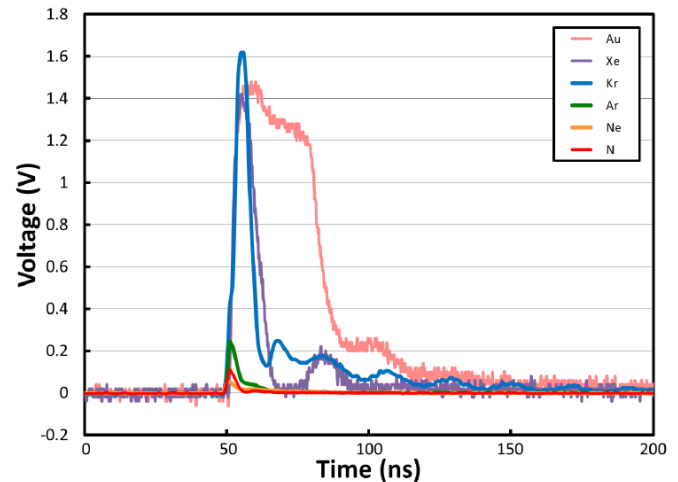


Fig.6. Worst case single-event transient observed with each ion when the LM6172 is irradiated in the voltage follower configuration and biased with 0 V on the input.

V. ACKNOWLEDGMENT

The authors gratefully acknowledge members of the Radiation Effects and Analysis Group who contributed to the test results presented here: Alyson D. Topper, Hak Kim, Anthony M. Phan, Donna J. Cochran, Donald K. Hawkins, James D. Forney, Christina M. Seidleck, Martin A. Carts, Edward P. Wilcox, and Stephen R. Cox. Special thanks go to Stephen P. Buchner and Dale McMorrow, Naval Research Laboratory for their excellent support of the laser testing, and thanks to Anthony B. Sanders for technical and editorial support.

VI. SUMMARY

We have presented current data from SEE testing on a variety of mainly commercial devices. It is the authors' recommendation that these data be used with caution. We also highly recommend that lot testing be performed on any suspect or commercial device.

VII. REFERENCES

- [1] Kenneth A. LaBel, Lewis M. Cohn, and Ray Ladbury, "Are Current SEE Test Procedures Adequate for Modern Devices and Electronics Technologies?," http://radhome.gsfc.nasa.gov/radhome/papers/HEART08_LaBel.pdf
- [2] Michael J. Campola, Donna J. Cochran, Alvin J. Boutte, Dakai Chen, Robert A. Gigliuto, Kenneth A. LaBel, Jonathan A. Pellish, Raymond L. Ladbury, Megan C. Casey, Edward P. Wilcox, Martha V. O'Bryan, Jean-Marie Lauenstein, Dan Violette, and Michael A. Xapsos, "Compendium of Current Total Ionizing Dose and Displacement Damage for Candidate Spacecraft Electronics for NASA," submitted for publication in IEEE Radiation Effects Data Workshop, Jul. 2015.
- [3] Michael B. Johnson, Berkeley Lawrence Berkeley National Laboratory (LBNL), 88-Inch Cyclotron Accelerator, Accelerator Space Effects (BASE) Facility <http://cyclotron.lbl.gov>.
- [4] B. Hyman, "Texas A&M University Cyclotron Institute, K500 Superconducting Cyclotron Facility," <http://cyclotron.tamu.edu/facilities.htm>, Jul. 2003.
- [5] W.J. Stapor, "Single-Event Effects Qualification," IEEE NSREC95 Short Course, sec. II, pp 1-68, Jul. 1995.
- [6] J. S. Melinger, S. Buchner, D. McMorrow, T. R. Weatherford, A. B. Campbell, and H. Eisen, "Critical evaluation of the pulsed laser method for single event effects testing and fundamental studies," IEEE Trans. Nucl. Sci., vol 41, pp. 2574-2584, Dec. 1994.
- [7] D. McMorrow, J. S. Melinger, and S. Buchner, "Application of a Pulsed Laser for Evaluation and Optimization of SEU-Hard Designs," IEEE Trans. Nucl. Sci., vol 47, no. 3, pp. 559-565, Jun. 2000.
- [8] JEDEC Government Liaison Committee, Test Procedure for the Management of Single-Event Effects in Semiconductor Devices from Heavy Ion Irradiation," JESD57, <http://www.jedec.org/standards-documents/docs/jesd-57>, Dec. 1996.
- [9] R. Koga and W. A. Kolasinski, "Heavy Ion-Induced Single Event Upsets of Microcircuits; A Summary of the Aerospace Corporation Test Data," IEEE Trans. Nucl. Sci., vol. 31, pp. 1190 – 1195, Dec. 1984.
- [10] NASA/GSFC Radiation Effects and Analysis home page, <http://radhome.gsfc.nasa.gov>
- [11] NASA Electronic Parts and Packaging (NEPP) web site, <http://nepp.nasa.gov/>.
- [12] Dakai Chen, Melanie Berg, Hak Kim, Edward Wilcox, Anthony Phan, Marco Figueiredo, and Ken LaBel "Heavy Ion Test Report for the RM24C128 EEPROM," 13-082a_LBNL 20140430_RM24C128, Apr. 2014.
- [13] Dakai Chen, Edward Wilcox, Hak Kim, Melanie Berg, and Ken LaBel, "Heavy Ion Test Report for the RM24EP64 EEPROM," 13-082b_LBNL20140917_RM24EP64, Sept. 2014.
- [14] Dakai Chen, Edward Wilcox, Melanie Berg, Hak Kim, Anthony Phan, Marco Figueiredo, Christina Seidleck, and Kenneth LaBel, "Single-Event Effect Performance of a Conductive-Bridge Memory EEPROM," submitted for publication in the IEEE Trans. Nucl. Sci., Dec. 2015.
- [15] Dakai Chen, Carl Szabo and Alyson Topper, "Heavy Ion Irradiation Test Report for the Samsung 850 PRO Series Solid State Drive," 14-055_T20141024_MZ7KE256HMHA, Oct. 2014.
- [16] D. Chen, H. Kim, A. Phan, E. Wilcox, K. LaBel, and S. Buchner, A. Khachatrian, and N. Roche, "Single-event effect performance of a commercial embedded ReRAM," IEEE Trans. Nucl. Sci., vol. 61, no. 6, pp. 3088–3094, Dec. 2014.
- [17] Megan Casey, Edward Wilcox, and Michael Xapsos, "Single-Event Transient Testing of the Texas Instruments LM6172 Dual Voltage Feedback Amplifier," 13-076_T20131218_T20140406_LM6172, Apr. 2014.
- [18] Michael Campola, Carolyn Thayer, John Doty, Edward Wilcox, "Single Event Effects Testing of a Commercial Off The Shelf Analog to Digital Converter in a Camera Link Application," 14-053-MiC-summary2015, Oct. 2014.
- [19] M. Campola, T. Wilcox, H. Kim, "Single Event Effect Testing of the Texas Instruments' MAX4595 Single-Channel Analog Switch," 14-077_T20141026_MAX4595, Oct. 2014.
- [20] M. Campola, T. Wilcox, H. Kim, "Single Event Effect Testing of the Maxim MAX308 8-Channel CMOS Analog Multiplexer," 14-061_T20141004_MAX308ESE, Oct. 2014.
- [21] Raymond Ladbury, "SEE Test Report for Texas Instruments TLV5618 2.7-V to 5.5-V Low-Power Dual 12-Bit Digital-to-Analog Converter with Power Down," 14-070_T20141025_TLV5618, Oct. 2015.
- [22] Raymond Ladbury, "SEE Test Report for Analog Devices ADP3330 High Accuracy, Ultralow IQ, 200 mA, SOT-23, anyCAP Low Dropout Regulator," 14-074_T20141026_ADP3330, Oct. 2015.
- [23] Raymond Ladbury, "SEE Test Report for Texas Instruments LMV7219 7 ns, 2.7 V to 5 V Comparator with Rail-to-Rail Output," 14-072_T20141026_LMV7219, Oct. 2015.
- [24] Raymond Ladbury, "SEE Test Report for Arizona Microtek AZ88923 High Speed Limiting Post Amplifier," 14-073_T20141024_AZ88923 Oct.2014.
- [25] Megan Casey, "Single-Event Transient Testing of the Crane Aerospace & Electronics SMHF2812D Dual DC-DC Converter," 14-021_TAMU20140404_SMHF2812, Apr. 2014.
- [26] J.-M. Lauenstein, M.C. Casey, E.P. Wilcox, A.D. Topper, and H. Kim, "Single-Event Effect Testing of the Cree CMF10120D SiC Power MOSFET" 12-080_LBNL20140919_CM F10120D, Sept. 2014.
- [27] Megan C. Casey, Jean-Marie Lauenstein, Raymond L. Ladbury, Edward P. Wilcox, Alyson D. Topper, Anthony Phan, Hak Kim, and Kenneth A. LaBel, "Schottky Diode Derating for Survivability in a Heavy Ion Environment," presented by Megan Casey at the IEEE Nuclear and Space Radiation Effects Conference (NSREC), Boston, MA, July 14, 2015.
- [28] M.C. Casey, E.P. Wilcox, A. Topper, H. Kim, "Single Event Testing of Diodes," T2013May-2014June_Diode, June 2014.
- [29] Melanie D. Berg, Kenneth A. LaBel, Jonathan A. Pellish, "Fail-Safe Strategies for FPGA Devices Targeted for Critical Applications," presented at the Single Event Effects (SEE) Symposium and the Military and Aerospace Programmable Logic Devices (MAPLD) Workshop, La Jolla, CA, Berg-SEEMAPLD2015-FPGA, May, 2015.
- [30] Melanie Berg, Kenneth LaBel, and Jonathan Pellish, "Single Event Effects in FPGA Devices 2014-2015," presented at NEPP-ETW, Berg-ETW2015-FPGA, Jun. 2015.
- [31] [Rodbell-2014] Kenneth P. Rodbell, Kevin G. Stawiasz, Michael S. Gordon, Phil Oldiges, Keunwoo Kim, Conal E. Murray, John G. Massey, Larry Wissel, Henry H. K. Tang, "Single Event Transients in 32 nm SOI Stacked Latches," E-5 talk presented at 2014 Nuclear and Space Radiation Effects Conference (NSREC), Paris, France, July 16, 2014.
- [32] Samsung Corporation Samsung 850 Pro Series SSD datasheet, http://www.samsung.com/global/business/semiconductor/minisit e/SSD/downloads/document/Samsung_SSD_850_PRO_Data_Sheet_rev_1_0.pdf, Aug. 2013.
- [33] Computer Aided INvestigative Environment (CAINE), <http://www.caine-live.net/>